

13-76-158-1
F-0258

Inclusive π^0 Production at Large Transverse Momentum
from $\pi^\pm p$ and pp Interactions at 100 and 200 GeV/c*

G. Donaldson, H. Gordon, K.-W. Lai, I. Stumer

Brookhaven National Laboratory, Upton, New York 11973

and

A. Barnes, J. Mellema, A. Tollestrup, R. Walker

California Institute of Technology, Pasadena, California 91109

and

O. Dahl, R. A. Johnson, A. Ogawa, M. Pripstein, S. Shannon

Lawrence Berkeley Laboratory, Berkeley, California 94720

* Work performed under the auspices of the U.S. Energy Research and
Development Administration.

By acceptance of this article, the publisher and/or recipient acknowledges the U.S. Government's
right to retain a nonexclusive, royalty-free license in and to any copyright covering this paper.

Inclusive π^0 Production at Large Transverse Momentum
from $\pi^\pm p$ and pp Interactions at 100 and 200 GeV/c*

G. Donaldson, H. Gordon, K.-W. Lai, I. Stumer

Brookhaven National Laboratory, Upton, New York 11973

and

A. Barnes, J. Mellema, A. Tollestrup, R. Walker

California Institute of Technology, Pasadena, California 91109

and

O. Dahl, R. A. Johnson, A. Ogawa, M. Pripstein, S. Shannon

Lawrence Berkeley Laboratory, Berkeley, California 94720

ABSTRACT

We have measured large transverse momentum (p_\perp) inclusive π^0 production at CM angles centered near 90° for $\pi^\pm p$ and pp interactions at 100 and 200 GeV/c. This is the first such measurement using a pion beam. The ratio $\sigma(pp \rightarrow \pi^0 X) / \sigma(\pi p \rightarrow \pi^0 X)$ decreases with increasing p_\perp and is independent of energy when expressed as a function of $x_\perp = p_\perp / p_{\max}$. We compare the data with predictions of various models.

* Work performed under the auspices of the U.S. Energy Research and Development Administration.

Particle production at large transverse momentum (P_{\perp}) is believed to result from the interaction of hadronic constituents.¹ A variety of single particle inclusive data from the CERN ISR² and from FNAL³ has been described with some success in terms of this hypothesis, but all of these were measurements of proton-proton or proton-nucleus interactions. To investigate the possible role of hadronic constituents in large p_{\perp} particle production, it is important to compare reactions produced by different incident particles having different internal structures. We report here the first measurement of inclusive π^0 production at large p_{\perp} using high energy pion beams, and compare these results with proton-induced data obtained under the same conditions.

The experiment was performed in the M2 beam at Fermilab. The apparatus (shown schematically in Fig. 1) consisted of two helium-filled differential Čerenkov counters, a series of beam defining counters, a 60 cm liquid hydrogen target, and a photon detector.⁴ Each of the Čerenkov counters was equipped with two phototubes which viewed two cones of light, thus allowing simultaneous π , K, and p identification. The beam defining counters excluded beam halo and double beam particles as well as most upstream interactions. Two hodoscopes measured the position and direction of the incident particle. The photon detector, a lead scintillator sandwich hodoscope of 70 horizontal and 70 vertical counters, contains 19 radiation lengths of lead interspersed with long narrow (73.5 x 1.05 cm) scintillator rods. Each counter (a group of 8 optically coupled rods) integrates the photon shower development along its direction of propagation. The hodoscope pulse heights give the transverse distributions of the energy deposited by all the photons hitting the detector.

The photon detector was displaced horizontally from the beam axis to have good acceptance for π^0 's in a region of CM angles from 50° to 110° . For triggering purposes, a weighted analog sum of the pulse heights in the vertical

counters of the detector was formed; this sum was roughly proportional to the total transverse momentum of the observed photons. When a sufficiently large p_{\perp} event was indicated, the pulse heights in all 140 counters were recorded on magnetic tape. The gains of the phototubes were monitored continuously during the experiment to an accuracy of about 1%.

By detailed off-line analysis of the pulse-height data, the position and energy of all photon showers in the detector were determined with a spatial resolution of ± 1 mm and energy resolution $\frac{\Delta E}{E} \approx 0.02 \sqrt{\frac{100 \text{ GeV}}{E}}$. Since this was an inclusive measurement, an event candidate was not rejected if more than two showers appeared in the detector; rather the photon pair having the largest P_{\perp} was selected.⁵ The resulting pair mass spectrum shows a clean π^0 peak as illustrated in Fig. 2(a). The background is composed of unassociated pairs of photons and/or charged particles. Its magnitude is on the average about 10% of the π^0 signal and has the same P_{\perp} dependence as the π^0 signal for all initial states. The resolution in mass is $\frac{\Delta M^2}{M^2} \approx 12\%$. The number of π^0 's within a given p_{\perp} interval was determined by fitting the mass spectrum for that interval (with target-empty contributions subtracted) to a Gaussian plus a linear background. The resulting invariant cross sections for $\pi^{\pm} p \rightarrow \pi^0 X$ and $pp \rightarrow \pi^0 X$ are given in Table I. In all three reactions the cross section at fixed p_{\perp} increases with increasing beam energy as shown in Fig. 2(b) for $\pi^{-} p \rightarrow \pi^0 X$. The cross section for $pp \rightarrow \pi^0 X$ is consistent with previous experiments.³

The principal objective of this experiment is a measurement of the ratios:

$$R(A/B) = \frac{E d\sigma/d^3 p (Ap \rightarrow \pi^0 X)}{E d\sigma/d^3 p (Bp \rightarrow \pi^0 X)}$$

where A and B are p, π^+ , or π^- . Results were obtained for each different reaction using the same apparatus, running conditions and analysis procedures so that this ratio would be insensitive to systematic errors affecting the individual cross sections; only the signature in the Cerenkov counters distinguished the reactions.⁶

The ratios $R(\pi^+/\pi^-)$ and $R(p/\pi^-)$ are presented in Fig. 3 as a function of p_{\perp} . At both 100 and 200 GeV/c, $R(\pi^+/\pi^-)$ is close to unity over the entire p_{\perp} region investigated. In contrast, $R(p/\pi^-)$ changes markedly between $p_{\perp} \sim 1$ and $p_{\perp} \sim 4$ GeV/c. At $p_{\perp} \sim 1$ GeV/c, the ratio is about 1.6, which is equal to the ratio of the total pp and π p cross sections. This can be understood by factorization arguments in the Mueller-Regge theory⁷ and has been observed before.⁸ However, the ratio decreases with increasing p_{\perp} , falling to a point where the π p cross section significantly exceeds the pp cross section at the largest measured p_{\perp} . In the highest p_{\perp} bin at each energy, a smooth extrapolation of our $pp \rightarrow \pi^0 + X$ data⁹ was made in order to compute the ratio.

Although the value of $R(p/\pi^-)$ at a fixed p_{\perp} is different at 100 and 200 GeV/c, $R(p/\pi^-)$ is independent of energy when expressed as a function of $x_{\perp} = p_{\perp}/P_{\max}$ as shown in Fig. 4. The pp and π p cross sections can be parameterized by a factorized function $E \frac{d\sigma}{d^3p} \propto (p_{\perp}^2 + M^2)^N (1-x_{\perp})^F$. The best fit gives $N_p = -5.4 \pm 0.2$, $M_p^2 = 2.3 \pm 0.3 \text{ GeV}^2$, $F_p = 7.1 \pm 0.4$ with $\chi^2/DF = 23/14$ for $pp \rightarrow \pi^0 X$, and $N_{\pi} = -5.0 \pm 0.1$, $M_{\pi}^2 = 1.8 \pm 0.2 \text{ GeV}^2$, $F_{\pi} = 5.5 \pm 0.3$ with $\chi^2/DF = 44/35$ for $\pi^{\pm} p \rightarrow \pi^0 X$. In the context of this parameterization both π p and pp interactions have approximately the same p_{\perp} dependence, and so the fall of $R(p/\pi)$ vs. x_{\perp} shown in Fig. 4 can be interpreted as the difference in the power of $(1-x_{\perp})$.

Under the assumption that large $p_{\perp} \pi^0$ production is dominated by quark-meson scattering ($qM \rightarrow qM$) or quark-antiquark annihilation ($q\bar{q} \rightarrow MM$), a simple application of the Constituent Interchange Model¹ predicts $F_p - F_{\pi} = 6$, in disagreement with our measured result of 1.6 ± 0.5 . Another parton model¹⁰ of the "quark fusion" type predicts a much smaller ratio $R(p/\pi)$ than is observed and hence is ruled out. If naively one thinks of the proton as having three constituents and the π as having two, then on the average the momentum of the constituents in the π should be larger than those in the proton. From this consideration

alone one would expect that the probability to produce a π^0 at large p_{\perp} would be somewhat larger for πp interactions than for pp interactions and that the difference between the two reactions should be in their x_{\perp} rather than their p_{\perp} dependence.

We would like to express our appreciation to Dr. R. Kenney for his continuing support and assistance throughout this experiment and to D. Hermeyer for his important contributions to the design and operation of the experiment. We gratefully acknowledge the cooperation of Dr. C. Brown and Dr. P. Koehler and many others at Fermilab.

TABLE I

Invariant cross sections $E \frac{d\sigma}{d^3p}$ (cm^2/GeV^2) at $\theta_{\text{cm}} = 90^\circ$ for the reactions $A p \rightarrow \pi^0 + X$ where $A = \pi^+, \pi^-$ and p .*

p_{\perp} Interval (GeV/c)	100 GeV/c			200 GeV/c		
	π^+	π^-	p	π^+	π^-	p
1.0-1.2	$(6.53 \pm 0.52) \times 10^{-29}$	$(6.70 \pm 0.54) \times 10^{-29}$	$(1.12 \pm 0.09) \times 10^{-28}$	$(9.78 \pm 0.78) \times 10^{-29}$	$(9.09 \pm 0.73) \times 10^{-29}$	$(1.31 \pm 0.10) \times 10^{-28}$
1.2-1.4	$(2.72 \pm 0.22) \times 10^{-29}$	$(2.59 \pm 0.21) \times 10^{-29}$	$(4.02 \pm 0.32) \times 10^{-29}$	$(3.71 \pm 0.30) \times 10^{-29}$	$(3.77 \pm 0.30) \times 10^{-29}$	$(5.92 \pm 0.47) \times 10^{-29}$
1.4-1.6	$(1.04 \pm 0.83) \times 10^{-29}$	$(8.57 \pm 0.69) \times 10^{-30}$	$(1.25 \pm 0.10) \times 10^{-29}$	$(1.62 \pm 0.13) \times 10^{-29}$	$(1.49 \pm 0.12) \times 10^{-29}$	$(2.13 \pm 0.17) \times 10^{-29}$
1.6-1.8	$(3.72 \pm 0.30) \times 10^{-30}$	$(3.41 \pm 0.27) \times 10^{-30}$	$(4.92 \pm 0.39) \times 10^{-30}$	$(6.44 \pm 0.52) \times 10^{-30}$	$(5.95 \pm 0.48) \times 10^{-30}$	$(8.82 \pm 0.71) \times 10^{-30}$
1.8-2.0	$(1.55 \pm 0.12) \times 10^{-30}$	$(1.44 \pm 0.12) \times 10^{-30}$	$(1.86 \pm 0.15) \times 10^{-30}$	$(3.16 \pm 0.25) \times 10^{-30}$	$(2.59 \pm 0.21) \times 10^{-30}$	$(3.86 \pm 0.31) \times 10^{-30}$
2.0-2.5	$(3.46 \pm 0.28) \times 10^{-31}$	$(3.07 \pm 0.25) \times 10^{-31}$	$(3.98 \pm 0.32) \times 10^{-31}$	$(5.93 \pm 0.47) \times 10^{-31}$	$(6.22 \pm 0.50) \times 10^{-31}$	$(8.57 \pm 0.69) \times 10^{-31}$
2.5-3.0	$(3.93 \pm 0.31) \times 10^{-32}$	$(3.83 \pm 0.31) \times 10^{-32}$	$(2.77 \pm 0.23) \times 10^{-32}$	$(1.21 \pm 0.10) \times 10^{-31}$	$(9.72 \pm 0.78) \times 10^{-32}$	$(1.23 \pm 0.10) \times 10^{-31}$
3.0-3.5	$(4.24 \pm 0.60) \times 10^{-33}$	$(4.0 \pm 0.6) \times 10^{-33}$	$(2.20 \pm 0.64) \times 10^{-33}$	$(1.81 \pm 0.23) \times 10^{-32}$	$(1.76 \pm 0.14) \times 10^{-32}$	$(1.57 \pm 0.13) \times 10^{-32}$
3.5-4.0	$(5.21 \pm 3.0) \times 10^{-34}$	$(8.6 \pm 3.1) \times 10^{-34}$		$(2.19 \pm 0.43) \times 10^{-33}$	$(2.68 \pm 0.21) \times 10^{-33}$	$(2.20 \pm 0.18) \times 10^{-33}$
4.0-4.5				$(9.0 \pm 3.0) \times 10^{-34}$	$(3.80 \pm 0.83) \times 10^{-34}$	$(2.42 \pm 0.80) \times 10^{-34}$
4.5-5.0					$(1.27 \pm 0.58) \times 10^{-34}$	

* The quoted error combines a point-to-point systematic uncertainty of 8% with the normal statistical contribution.

Not included in the quoted error is an additional 5% uncertainty in overall normalization and an uncertainty of

3% in the p_{\perp} scale.

REFERENCES

1. For example: R. Blankenbecler, S. C. Brodsky and J. Gunion SLAC-PUB-1585, Stanford Linear Accelerator Center (1975).
2. For example: F. W. Büsser, et al., Phys. Lett. 46B, 471 (1973), M. Banner, et al., Phys. Lett. 44B, 537 (1973), and B. Alper, et al., Phys. Lett. 44B, 521 (1973); 44B, 527 (1973).
3. For example: D. C. Carey, et al., Phys. Rev. Lett. 33, 327 (1974), J. W. Cronin, et al., Phys. Rev. D11, 3105 (1975), and J. A. Appel, et al., Phys. Rev. Lett. 33, 719 (1974).
4. The detector and other apparatus were used in a previous experiment on $\pi^- p$ charge exchange and are described in A. V. Barnes, et al., Proceedings of the SLAC Summer Institute on Particle Physics, July 29-August 10, 1974, SLAC-179, Vol. I, p. 1, and R. Johnson, LBL-4610 (Ph.D. thesis, unpublished) (1975).
5. Because of the steep falloff of the photon spectra with increasing p_{\perp} , we find that our neglect of the photon pairs with lower p_{\perp} causes an error of less than 2% in the measured invariant cross sections.
6. The contamination in the p and π^+ samples from misidentified particles is $\leq 0.5\%$. In the π^- sample the contamination is $\leq 0.1\%$.
7. A. H. Mueller, Phys. Rev. D2, 2963 (1970).
8. J. Erwin, et al., Phys. Rev. Lett. 33, 1352 (1974).
9. This extrapolation is consistent with the measurements in References 2 and 3.
10. B. L. Combridge, Phys. Rev. D10, 3849 (1974).

FIGURE CAPTIONS

Fig. 1 Schematic view of apparatus--not to scale.

Fig. 2(a) Mass spectrum of two photon combinations for $2.0 < p_{\perp} < 2.5$ GeV/c from $\pi^- p$ interactions. For events with more than two photons in the detector, the pair with the largest p_{\perp} is plotted.

(b) The invariant cross section versus p_{\perp} for the reaction $\pi^- p \rightarrow \pi^0 X$ at 100 and 200 GeV/c and CM angles near 90° .

Fig. 3 Ratios of invariant cross sections as described in the text versus p_{\perp} .

Fig. 4 Ratio of invariant cross sections versus x_{\perp} for $pp \rightarrow \pi^0 X$ and $\pi^- p \rightarrow \pi^0 X$ at 100 and 200 GeV/c.

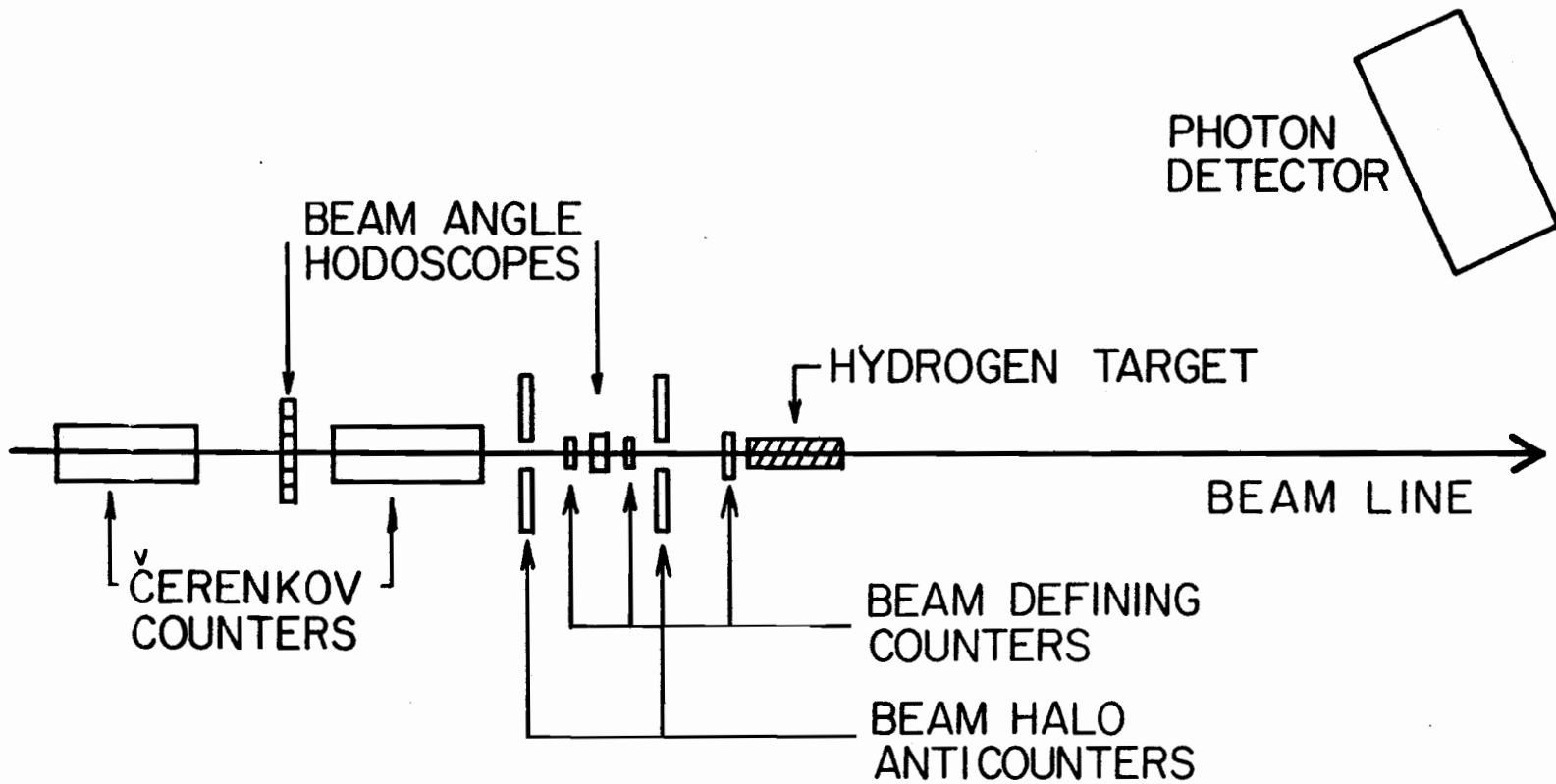


Fig. 1

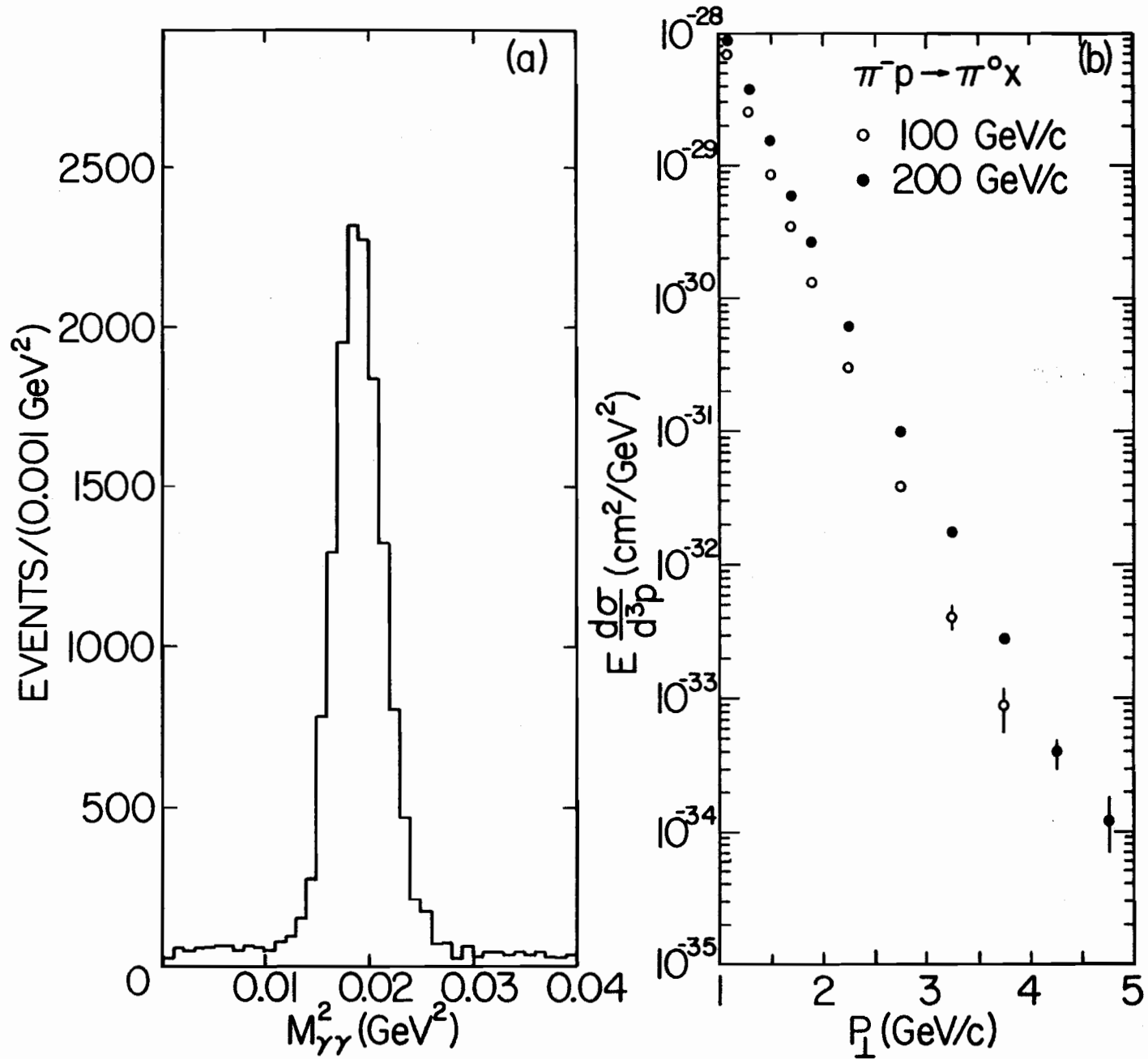


Fig. 2

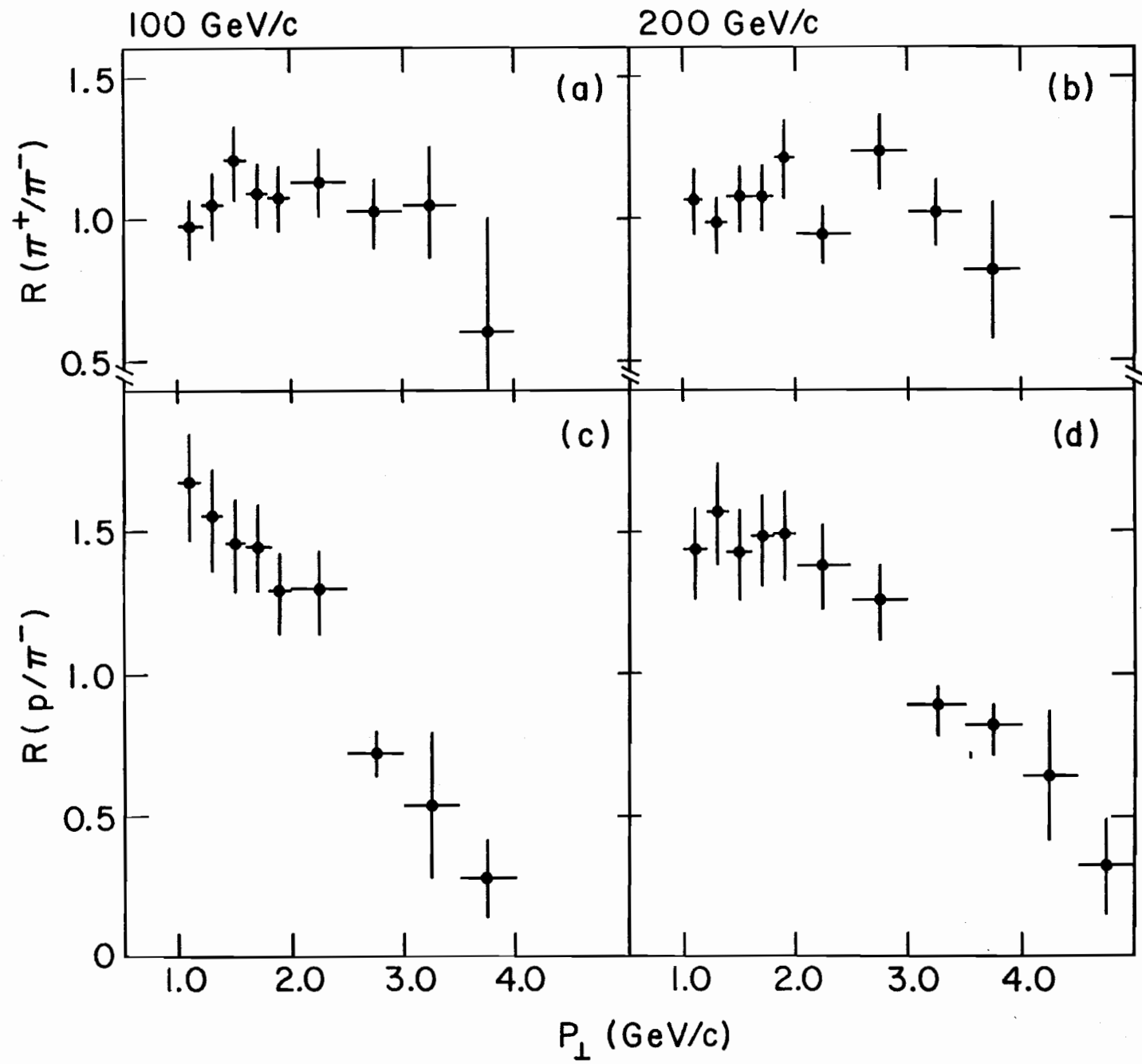


Fig. 3

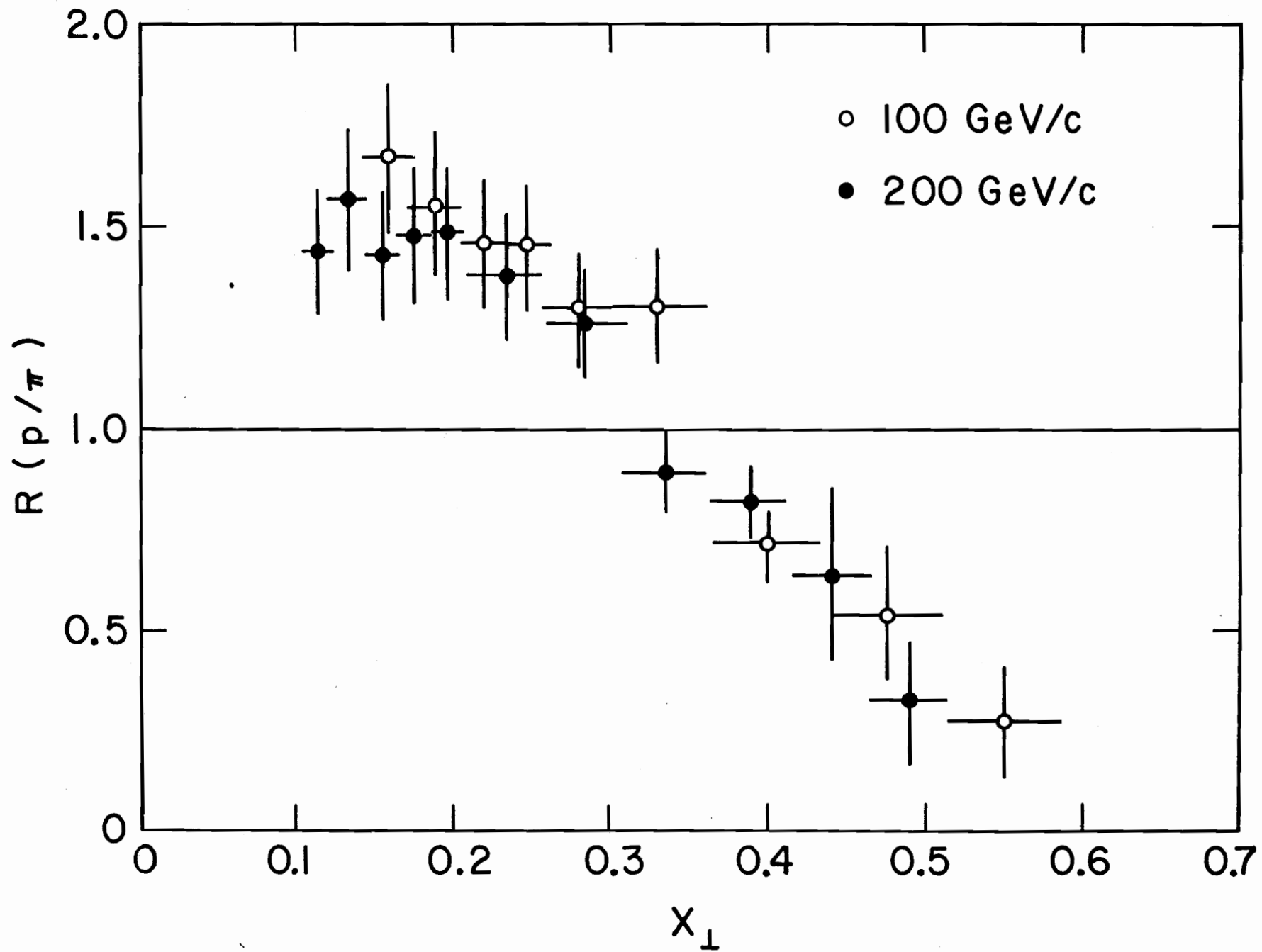


Fig. 4